Pulsed blue light inactivates two strains of human coronavirus

Chukuka S. Enwemeka [a, *], Violet V. Bumah [a], John L. Mokili [b]

[a] College of Health and Human Services, San Diego State University, San Diego, CA, USA
[b] Viral Information Institute, Department of Biology, College of Sciences, San Diego State University, San Diego, CA, USA

ARTICLE INFO

ABSTRACT

Emerging evidence suggests that blue light has the potential to inactivate viruses. Therefore, we investigated the effect of 405 nm, 410 nm, 425 nm and 450 nm pulsed blue light (PBL) on human alpha coronavirus HCoV-229 E and human beta coronavirus HCoV-OC43, using Qubit fluorometry and RT-LAMP to quantitate the amount of nucleic acid in irradiated and control samples. Like SARS-CoV-2, HCoV-229E and HCoV-OC43 are single stranded RNA viruses transmitted by air and direct contact; they have similar genomic sizes as SARS-CoV-2, and are used as surrogates for SARS-CoV-2. Irradiation was carried out either at 32.4 J cm^{-2} using 3 mW cm^{-2} irradiance or at 130 J cm^{-2} using 12 mW cm^{-2} irradiance. Results: (1) At each wavelength tested, PBL was antiviral against both coronaviruses. (2) 405 nm light gave the best result, yielding 52.3% (2.37 log$_{10}$) inactivation against HCoV-OC43 ($p < .0001$), and a significant 1.46 log$_{10}$ (44%) inactivation of HCoV-229E ($p < .01$). HCoV-OC43, which like SARS-CoV-2 is a beta coronavirus, was more susceptible to PBL irradiation than alpha coronavirus HCoV-229E. The latter finding suggests that PBL is potentially antiviral against multiple coronavirus strains, and that, while its potency may vary from one virus to another, it seems more antiviral against beta coronaviruses, such as HCoV-OC43. (3) Further, the antiviral effect of PBL was better at a higher irradiance than a lower irradiance, and this indicates that with further refinement, a protocol capable of yielding 100% inactivation of viruses is attainable.

1. Introduction

Coronaviruses are notorious for wrecking pandemics of epic proportion [1–3], as evidenced by the global spread of novel coronavirus SARS-CoV-2, the cause of COVID-19 disease which has infected more than 172 million, killed over 3.7 million, and caused untold socioeconomic havoc worldwide [4]. The familiar world response to disease pandemics has been vaccine development and deployment, which though effective in boosting immunity and reducing the severity of disease, does not inactivate and clear viruses from the environment. Vaccines effectively enable humanity to better cope with diseases, and this is evidenced by the annual epidemics of several viral diseases for which vaccines have been available for decades [5,6]. For example, there have been vaccines for the common cold coronavirus and flu [5,6], but during the last three recent cold/flu seasons (2016–17, 2017–18, and 2018–19), the United States Centers for Disease Control (CDC) recorded over 105 million infections and more than 133,000 deaths in the US alone [5,6].

Vaccine development is not just expensive; it takes tedious years of research to develop potent new vaccines. Even then, each vaccine must be modified regularly to help overcome evolving new strains of coronaviruses. This applies to endemic coronavirus diseases, such as Severe Acute Respiratory Syndrome (SARS), Middle East Respiratory Syndrome (MERS), emerging variants of COVID-19, and other epidemic and pandemic seasonal viral diseases. This scenario suggests the need for a paradigm shift, and new ways to combat the severity and spread of coronavirus infections.

Emerging evidence indicates that blue light inactivates bacteria and viruses and has great potential to inactivate coronaviruses [7–32]. Light in the blue spectrum inactivates baculoviruses [7], leukemia virus [8], herpes simplex virus [9], human immunodeficiency virus [10] and the flu virus [11]. For example, in a definitive study, Richardson and Porter [7] compared the infectivity of murine leukemia virus stored in darkness versus those exposed to visible light and showed that exposure to light significantly reduced virus infectivity. The effect was not due to ultraviolet rays (UV), because after filtering out UV to eliminate its antiviral effect, they found that blue 420–430 nm light inactivated the virus. This finding is significant because it shows that UV is not a sine qua non in

---

virus inactivation. In further experiments, they found that an endogenous or exogenous chromophore or photosensitizer was not necessary to inactivate the virus, and that the integrity of the virus particle and envelope were unaffected by light; rather, the loss of infectivity occurred because irradiation impaired the reverse transcription process [7]. A clear implication of the latter finding is that the virion-associated reverse transcription complex is photo-labile and susceptible to inactivation by blue light.

Further evidence, supporting the use of blue light as a potential antiviral against coronaviruses, comes from a recent study of the effect of broad-spectrum light on aerosolized flu virus. Using the decay constant and half-life of the virus as indices of virus survival, Schuit et al. [11] showed that simulated sunlight alone significantly inactivated the virus, resulting in 0.29 ± 0.09 min^{-1} decay constant and a half-live of approximately 2.4 min compared to non-irradiated control, which had 0.02 ± 0.06 min^{-1} decay constant and 31.1 min half-life. Exposure to light resulted in a 93% increase in decay constant and a concomitant 92.3% decline in the half-life of the virus [11]. Given the close relationship between coronaviruses and the flu virus, their finding further suggests that blue light has the potential to inactivate coronaviruses.

Recently, we showed that pulsed blue light [PBL] inactivates bacteria at ultralow irradiances 40 to 100 times more than higher irradiances of continuous wave (CW) blue light [12–14], which itself inactivates numerous Gram-positive and Gram-negative bacteria [15–32]. The foregoing evidence that CW blue light inactivates certain viruses, and our finding that PBL is significantly more potent than CW blue light, prompted us to test the effect of PBL on two coronavirus strains—human alpha HCoV-229E and human beta HCoV-OC43. These two viruses are endemic in humans and remain responsible for 15–30% respiratory tract infections every year, even though they were first isolated more than 50 years ago [33]. Like SARS-CoV-2, the virus responsible for the pandemic of COVID-19 disease, the two viruses are single stranded RNA viruses transmitted by air and direct contact. Their genomic sizes are similar to SARS-CoV-2 [34], and HCoV-OC43 is of the same beta coronavirus genus as SARS-CoV-2. For these reasons, HCoV-OC43 and HCoV-229E viruses have been used as surrogates for SARS-CoV-2 [35].

The need for a paradigm shift in embracing hitherto ill-explored ways to combat coronavirus infections cannot be overemphasized. Humanity cannot afford to continuously rely mainly on vaccines to cope with epidemics and pandemics of coronavirus infections, given continual evolution of diverse strains and the resulting morbidity and mortality which, if unabated, would continue ad infinitum. If PBL proves to be a safe way to inactivate coronaviruses, it could advance efforts to eradicate the virus, stem future pandemics, and trigger the evolution of PBL-based technologies that could be used to clear the environment of coronaviruses. Moreover, since PBL is antimicrobial against several bacteria, it could inactivate many of the opportunistic bacteria associated with coronavirus diseases as well and minimize the impact of infection. Our previous successes in inactivating multiple strains of the same bacterium [16,17,32], also suggest that PBL may be effective in stemming current and emerging coronavirus strains.

2. Materials and Methods

2.1. Experimental design and treatment

The viruses were obtained from the American Type Culture Collection (ATCC), already cultured in RPMI-1640 Medium (ATCC catalogue number 30–2001™) containing 2 mM L-glutamine, 10 mM HEPES, 1 mM sodium pyruvate, 4500 mg/L glucose, and 1500 mg/L sodium bicarbonate, for use in incubators using 5% CO_2 in air. As shown in Fig. 1., titers of 5×10^3 PFU/mL of alpha human coronavirus HCoV-229E and beta human coronavirus HCoV-OC43, ATCC® VR1558™ and VR-740, respectively, were placed in separate 6 well plates and then irradiated perpendicularly at a distance of 2.3 cm, with 405, 410, 425 and 450 nm PBL. The two sets of irradiation experiments were performed in enclosed chambers in our BSL-2 facility as approved by the Institutional Biosafety Committee of San Diego State University, approval number BUA #20-07-008E.

First, aliquots of 140 μL of 5×10^3 PFU mL^{-1} of each virus were transferred into the two center wells of the six-well plates and irradiated with either 405, 410, 425 or 450 nm PBL using 3 mW/cm^2 irradiance and a dose of 32.4 J/cm^2. In a second series of experiments, aliquots of 140 μL of 5×10^3 PFU mL^{-1} of each virus were transferred into the two center wells of another set of six-well plates and irradiated with a higher dose of 130 J/cm^2, using 12 mW/cm^2 incident irradiance of each wavelength. Non-irradiated plates, prepared and handled under identical conditions, served as controls. With each wavelength, the experiments were repeated four times. Viral RNA was then extracted and
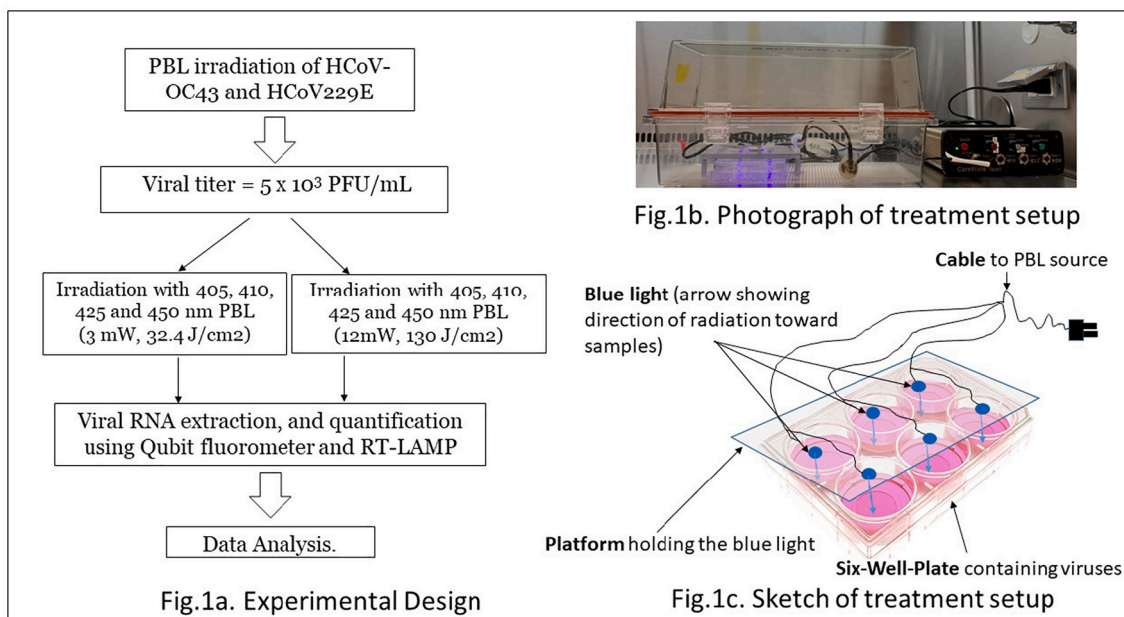

Fig. 1. Experimental design and set up.

quantified using a Qubit fluorometer and qPCR RT-LAMP as detailed below.

2.2. Pulsed blue light device

Custom made 405, 410, 425 and 450 nm LED devices (Carewear Corp), calibrated to yield irradiance of 3 or 12 mW/cm^2 at the surface of the viral samples, were used for this study. The accuracy of irradiance produced by each device in pulsed mode was $+/-$ 3% as measured with an integrating sphere and a spectrometer. Pulsing was set at 33% duty cycle—i.e., light was on 33% of the time and off 67% of the time during each pulse cycle. The full spectral width of each wavelength was ±10 nm approximately. The 3 mW/cm^2 device had 1500 25 μm sized LEDs printed on a flexible 125 μm polyethylene terephthalate (PET) film, while the 12 mW/cm^2 device was composed of conventional high efficiency LEDs mounted on a plastic holder. In previous experiments, we have used the 450 nm PBL version of these novel light technologies to inactivate several bacteria [13–15] and have ascertained that the device did not generate any detectable amount of heat during irradiation.

2.3. Viral quantification

Following irradiation, viral RNA was extracted using Qiagen QIAamp viral RNA kit and the concentration of the extracted RNA determined using a Qubit fluorometer. Secondarily, we used WarmStart RT-LAMP (Reverse Transcriptase Loop-Mediated Isothermal Amplification) protocol (New England Biolabs, Inc.) to determine the amount of RNA in treated and control specimens.

2.3.1. Nucleic acid extraction

RNA from irradiated and non-irradiated viruses were extracted using the QIAamp viral RNA kit (QIAGEN, Valencia, CA) as per manufacturer's instructions. Briefly, all samples (approximately 140 μL) were placed in separate DNase/RNase free 1.5 mL Eppendorf tubes and lysed under highly denaturing conditions by adding 560 μL of lysis buffer to inactivate RNases and to ensure isolation of intact viral RNA. This mixture was pulsed-vortexed for 15 s, incubated at room temperature for 10 min, and briefly centrifuged to remove drops from the lid of the tubes. Then, 560 μL of ethanol (96–100%) was added, pulsed vortexed for another 15 s before loading 630 μL of the samples unto the QIAamp Mini spin column containing a silica-based membrane. The spin columns were centrifuged at 6000 x*g* (8000 rpm) for 1 min and the filtrate discarded. The rest of the sample was then added to the column, centrifuged at the same speed for 1 min and the filtrate discarded. This process allowed the RNA to bind to the membrane; the contaminants were then washed away by adding 500 μL wash buffer 1 and centrifuging at 6000 × g (8000 rpm) for 1 min. A second 500 μL wash buffer (wash buffer 2) was then added to the column and centrifuged at full speed (20,000 × g, 14,000 rpm) for 3 min. The column was then placed in a clean DNase/ RNase free 1.5 mL microcentrifuge tube and 40 μL of buffer AVE (RNase-free water containing 0.04% sodium azide, elution buffer) added and allowed to equilibrate at room temperature for 1 min before centrifuging at 6000 × g (8000 rpm) for 1 min. Another 40 μL of buffer AVE was added to the column and the elution process repeated. The high-quality RNA eluted, was quantified immediately using Qubit fluorometer or LAMP qPCR; alternatively, the sample was stored at −20 °C or − 80 °C for use later.

2.3.2. Fluorometric determination of RNA concentration

The Qubit fluorometer uses fluorescent dyes that emit signals only when bound to the specific target molecules (DNA or RNA) even in the presence of free nucleotides, degraded nucleic acids, or protein contaminants. To determine RNA concentration, 2 μL of extracted RNA from both irradiated and non-irradiated groups were separately placed in thin-wall, clear 0.5 mL PCR tubes containing 198 μL of Qubit working solutions. Qubit RNA standards in tris-EDTA (TE) buffer were prepared separately by adding 10 μL of standard 1 to 190 μL of working solution or 10 μL of standard 2 to 190 μL working solution. Then, each standard was inserted into the Qubit fluorometer along with tubes containing extracted RNA from each sample to determine their respective RNA concentration in ng/mL.

2.3.3. WarmStart RT-LAMP assay

The WarmStart RT-LAMP test is a simple ultrasensitive assay based on a one-step Loop-Mediated Isothermal Amplification (LAMP) of RNA targets. The RT-LAMP uses isothermal amplification techniques that provide rapid detection of a target nucleic acid using LAMP-specific primers and a strand-displacing DNA polymerase and has been used previously to detect SARS-CoV-2. The kit (New England Biolabs) contains the WarmStart LAMP 2× master mix, which is a blend of BST 2.0 WarmStart DNA polymerase and WarmStart RTx (reverse transcriptase) in an optimized LAMP buffer solution. Eppendorf tubes were used for the assay. Briefly, each experimental tube, contained a set of six primers (below) for the gene of interest, 12.5 μL WarmStart LAMP Master Mix, 1.5 μL fluorescent dye, 2.5 μL (10×) LAMP Primer Mix, 2 or 4 μL of target RNA, and the remaining volume made up to 25 μL with H$_2$O. The tubes were then placed in the Rotor-Gene Q thermocycler (QIAGEN) and set at 65 °C for 30 min to perform the one-step reverse transcription to cDNA and real-time PCR of viral nucleocapsid genes of each of the two coronavirus strains using the following primers:

HCoV OC43:

OC43_F3: AGT CCC AGC TAC TGA AGC T; OC43_B3: TGA CAT CAG CCT GGT TGC; OC43_ FIP: GGC AGC AGT TGA CGC TGG TT- GGG GTA CTG GTA CAG ACA CA; OC43_BIP: ACT ATC TGG GAA CAG GAC CGC A-C GAC CCA GTA GAC TCC GTT; OC43_F2: GGG GTA CTG GTA CAG ACA CA; OC43_B2: CGA CCC AGT AGA CTC CGT T.

HCoV 229E:

229E_F3: CCC ATC AAC AAG AAA GAC AA; 229E_B3: ATC AAC AGC AAC CCA GAC; 229E_FIP: CAC CCG TTT GCC CTT TCT AGT T-AA TAA GCT TAT AGG CTA TTG GAA TG; 229E_BIP: GTC ACC CAA GCT GCA TTT TTA TT- CAC CTT CAA CAC GCT CTC; 229E_F2: AAT AAG CTT ATA GGC TAT TGG AAT G; 229E_B2: CAC CTT CAA CAC GCT CTC.

The quantification cycle (Cq) value, i.e., the number of cycles required for the fluorescent signal to exceed the background fluorescence—also referred to as threshold cycle (Ct), crossing point (Cp), or take-off point (TOP)—was used to estimate the amount of RNA present in both irradiated and non-irradiated viruses; this corresponds to the amount of HCoV-OC43 or HCoV-229E present in the samples. Lower C$_q$ values indicate high amounts of the target sequence. Higher C$_q$ values signify lower amounts of target nucleic acid.

2.4. Data analysis

Descriptive statistics, i.e., means, standard deviations of means and standard errors, reflecting RNA concentration and the quantified amount of cDNA amplification obtained were summarized and subjected to inferential statistical analysis using SPSS. Then for each virus, using wavelength, treatment group, irradiation dose as factors, a multivariate analysis of variance (and where appropriate, ANOVA) was used to determine groups that differ in outcome. Then, Bonferroni *post-hoc* procedure was used to pinpoint statistical differences between controls and treated samples based on each factor. Data were graphed to ease interpretation and visualization.

3. Results

3.1. The effect of PBL on human coronavirus HCoV-OC43 RNA concentration

Irradiation with PBL significantly reduced HCoV-OC43 RNA concentration ($p < .05$). The effect was more pronounced in viral samples irradiated with 405 nm wavelength. Following PBL irradiation at 3 mW/

cm^2 irradiance and 32.5 J/cm^2 fluence, the mean concentrations of RNA extracted were $138.5 \times 10,^2$ $174.2 \times 10,^2$ $194.3 \times 10,^2$ or 184.2; $\times 10^2$ ng/mL for samples irradiated with 405 nm, 410 nm, 425 nm, or 450 nm wavelengths, respectively, compared to 242.3×10^2 ng/mL for the non-irradiated control (Fig. 2a). As shown in Fig. 2b, irradiation with 405 nm PBL inactivated HCoV-OC43 44.7%, compared to 34.2%, 19.8%, 28.8% and 0% for 410 nm, 425 nm, 450 nm and non-irradiated control, respectively.

Increasing the irradiance from 3.0 mW/cm^2 to 12 mW/cm^2 and raising the fluence from 32.4 J/cm^2 to a dose of 130 J/cm^2 enhanced the antiviral effect of PBL significantly at each wavelength ($p < .0001$). The mean RNA concentration of irradiated HCoV-OC43 were 125×10^2 ng/mL, 128.8×10^2 ng/mL, 130.8×10^2 ng/mL and 152.5×10^2 ng/mL, respectively for samples treated with 405 nm, 410 nm, 425 nm, and 450 nm PBL. The corresponding RNA concentration for control non-irradiated samples was 262×10^2 ng/mL, Fig. 2c. These values

correspond to 52.3%, 50.9%, 50.1% and 41.8% viral inactivation following treatment with 405 nm, 410 nm, 425 nm, and 450 nm PBL, respectively (Fig. 2d). Viral inactivation was 0% in non-irradiated control samples. While these data again show that treatment with 405 nm gave the best results 52.3% or 2.37 $\log_{10}$ inactivation ($p < .0001$), they show that increasing the irradiance and dose of 410 nm, 425 nm and 450 nm PBL result in significantly more viral inactivation compared to the lower dose level, even for these longer wavelengths, Fig. 2d. For example, irradiation with 410 nm, 3 mW/cm^2 at 32.4 J/cm^2 produced a 34.18% inactivation, while irradiation at the same 410 nm wavelength using 12 mW/cm^2 irradiance and 130 J/cm^2 fluence gave 50.9% inactivation, a 16.7% improvement in viral inactivation. This observation was substantiated when, in a test experiment, we irradiated HCoV-OC43 at three increasing doses, 32.4 J/cm^2, 64.8 J/cm mW/cm^2 and 130 J/cm mW/cm^2. As shown in Fig. 2e and f, viral inactivation increased progressively with increasing doses. Thus, these findings suggest that
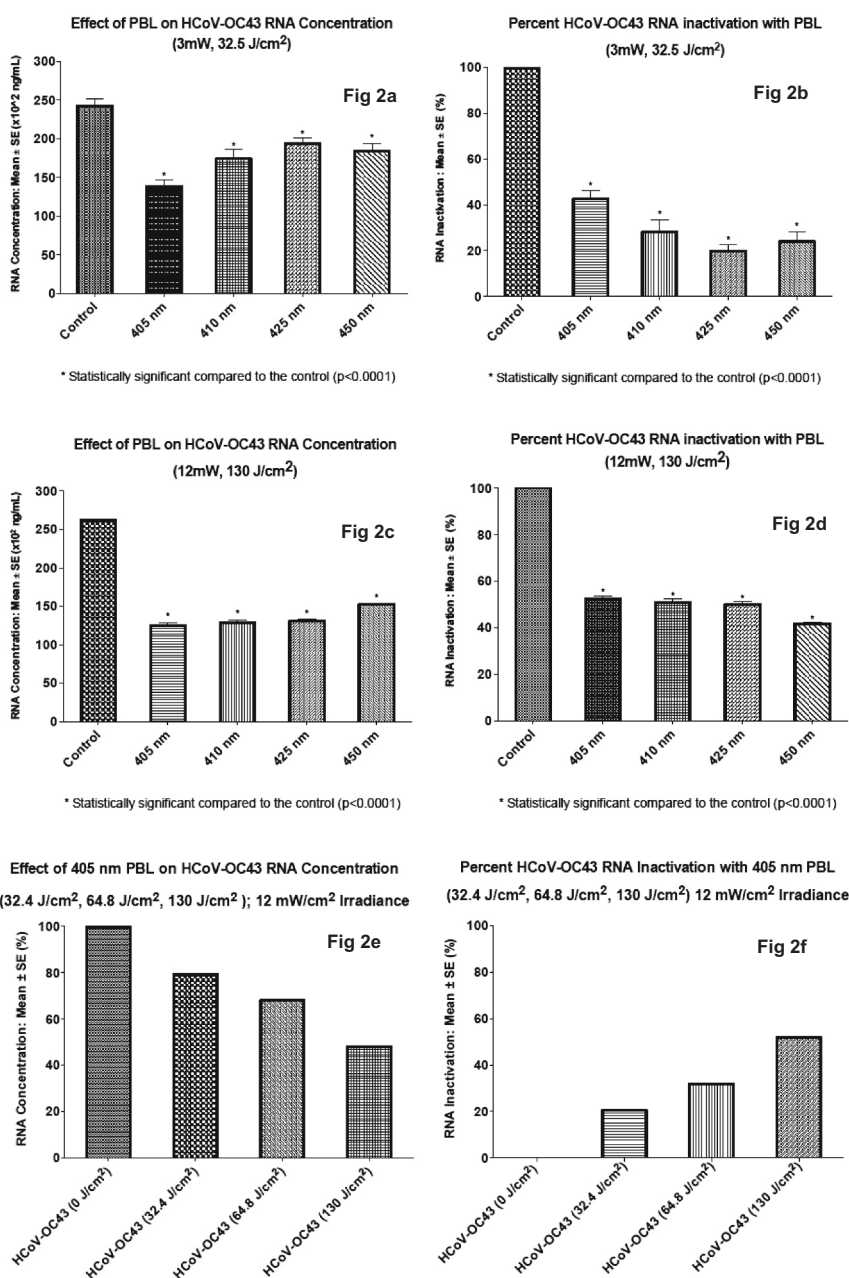

Fig. 2. The effect of PBL on HCoV-OC43 RNA concentration.

higher irradiances, and perhaps further refinement of the irradiation parameters could yield 100% inactivation of coronavirus HCoV-OC43.

3.2. The effect of PBL on human coronavirus HCoV-229E RNA concentration

Overall, PBL irradiation of HCoV-229E gave similar results as irradiation of HCoV-OC43; however, viral inactivation at each wavelength and at each dose level was less. This overall finding suggests that HCoV-OC43 is more susceptible to PBL than HCoV-229E; however, more data are needed to confirm this observation. The RNA concentrations of irradiated HCoV-229E were 46.7×10^2 ng/mL, 42.7×10^2 ng/mL, 56.3×10^2 ng/mL and 50.0×10^2 ng/mL, respectively for samples irradiated with 405 nm, 410 nm, 425 nm and 450 nm PBL using 3 mW/cm^2 irradiance and 32.5 J/cm^2 fluence. The non-irradiated control value was 69.1×10^2 ng/mL. Irradiation with 410 nm PBL inactivated HCoV-229E the most, 38.2% followed by 405 nm wavelength (32.4%). The difference between the potency of both wavelengths falls within the limits of experimental error. Percent inactivation for 405 nm, 425 nm, 450 nm and non-irradiated control was 32.4%, 18.6%, 27.7% and 0% respectively.

Increasing irradiance from 3 mW/cm^2 to 12 mW/cm^2 and dose from 32.4 J/cm^2 to 130 J/cm^2 enhanced the antiviral effect of PBL, yielding 37.7×10^2 ng/mL, 39.8×10^2 ng/mL, 43.1×10^2 ng/mL and 45.9×10^2 ng/mL RNA concentration for each of 405 nm, 410 nm, 425 nm and 450 nm PBL. The corresponding control value was 67.1×10^2 ng/mL. Thus, percentage inactivation was 43.8%, 40.7%, 35.6% and 31.5% for 405 nm, 410 nm, 425 nm and 450 nm PBL respectively, compared to 0% for non-irradiated control. As with inactivation of HCoV-OC43, 405 nm PBL was more antiviral against HCoV 229E, it gave 1.46 log $_{10}$ (43.8%) inactivation, ($p < .0001$); Fig. 3d.

3.3. WarmStart RT-LAMP of HCoV-OC43

RT-LAMP was used to quantify the amount of RNA present in PBL irradiated viruses. As shown in Table 1a, irradiation with 405 nm PBL gave the highest Cq value, 20.74, indicating that samples irradiated with this wavelength had the lowest amount of nucleic acid. The Cq value for control non-irradiated HCoV-OC43 was 15.13, while the values for samples irradiated with 450 nm, 425 nm, and 410 nm were 17.97, 16.68 and 19.53, respectively. Doubling the starting RNA concentration from 2 μL to 4 μL before amplification did not make a significant difference; the Cq value for the control non-irradiated virus was 15.56, while the values for each of 450 nm, 425 nm, 410 nm and 405 nm PBL were 17.41, 17.82, 18.53 and 19.51, respectively (Table 1b). In each case, the non-template controls remained at baseline.
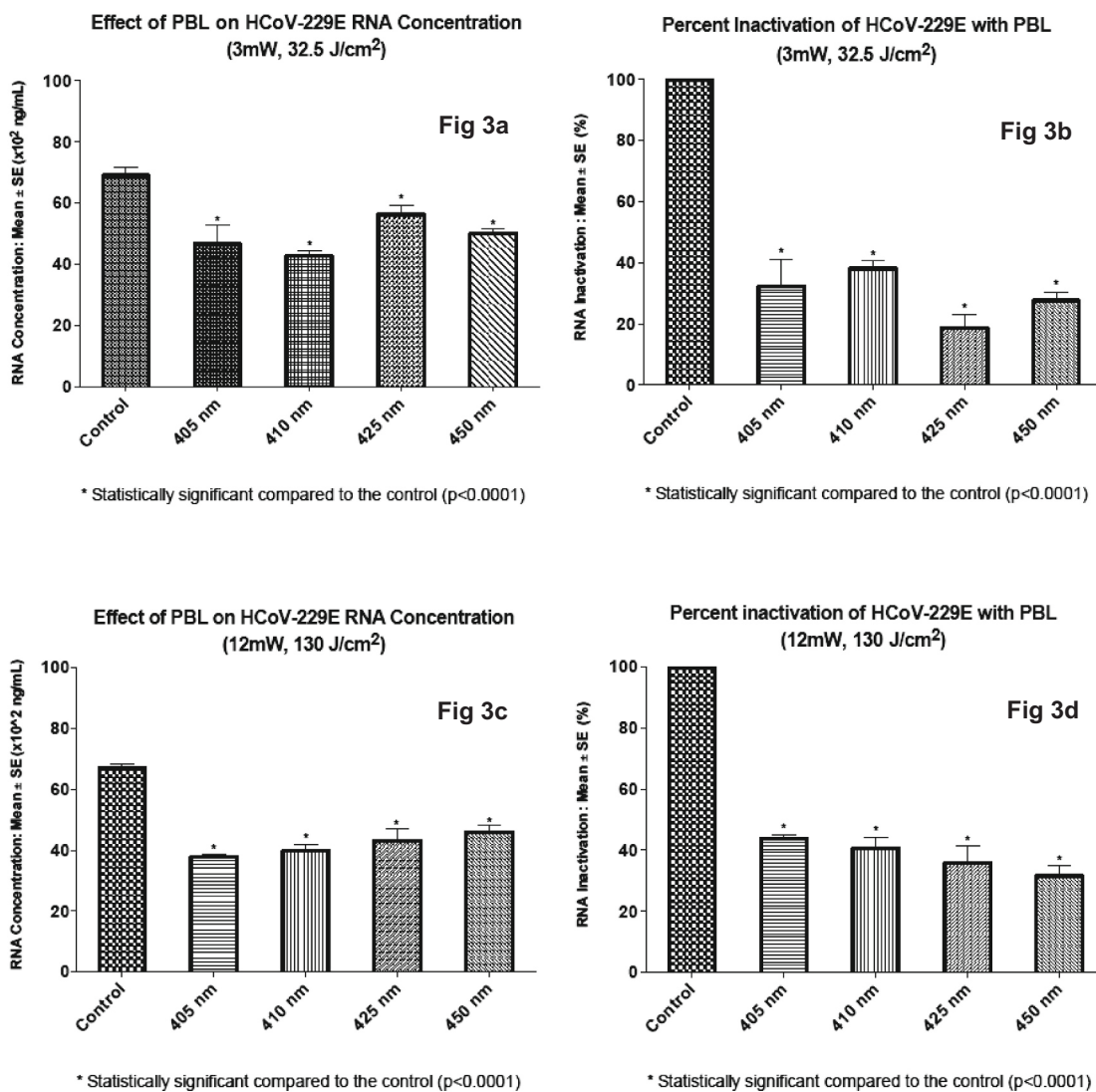

Fig. 3. The effect of PBL on HCoV-229E RNA concentration.

Table 1
RT-LAMP of PBL irradiated HCoV-OC43 (2 μL RNA).

Sample name	Cq	Take-off
a)		
405 nm	20.74	20.60
410 nm	19.53	19.40
425 nm	16.68	16.20
450 nm	17.97	17.70
Non-irradiated Control	15.13	14.50
b) RT-LAMP of PBL irradiated HCoV-OC43 (4 μL RNA)		
405 nm	19.15	19.10
410 nm	18.53	18.10
425 nm	17.82	17.60
450 nm	17.41	17.20
Non-irradiated Control	15.56	15.10

3.4. WarmStart RT-LAMP of HCoV-229E

PBL irradiation of HCoV-229E coronavirus gave similar results as reported for HCoV-OC43; overall, the results show decreased amounts of RNA following irradiation. The non-irradiated control viral RNA (2 μL) had a Cq of 16.35, compared to 18.32, 17.89, 19.26 and 20.03 for 450, 425, 410 and 405 nm respectively (Table 2a). When the volume of amplified RNA was doubled to 4 μL, similar values of Cq were observed; the values were 16.11, 17.65, 18.85, 19.79 and 19.81 for non-irradiated control, 450 nm, 425 nm, 410 nm and 405 nm PBL, respectively (Table 2b).

4. Discussion

Our results demonstrate the antiviral potential of PBL against human coronaviruses HCoV-OC43 and HCoV-229E. The data show that: (1) each wavelength of PBL tested is antiviral against the two coronaviruses, and (2) 405 nm gave the best result yielding 52.3% (2.37 $\log_{10}$) inactivation against HCoV OC43 ($p < .0001$), and a significant 1.46 $\log_{10}$ (44%) inactivation of HCoV-229E ($p < .01$). HCoV OC43 was more susceptible to irradiation with PBL than HCoV-229E. This finding suggests that the antiviral effect of PBL vary with each virus strain; it equally shows that PBL is potentially antiviral against multiple coronavirus strains, in particular, beta coronaviruses, such as HCoV-OC43. This evidence that PBL inactivates two surrogates of the deadly coronavirus SARS-CoV-2—the virus responsible for the devastating pandemic of COVID-19 disease, is quite significant. Like SARS-CoV-2, HCoV-229E and HCoV-OC43 are single stranded RNA viruses transmitted by air and direct contact; they have similar genomic sizes as SARS-CoV-2, hence they are used as surrogates for SARS-CoV-2 [35]. HCoV-OC43 is more closely related to SARS-CoV-2; the two are beta coronaviruses of the same genus, while HCoV-229E is an alpha coronavirus. Therefore, the superior antiviral effect of PBL on HCoV-OC43, suggests that SARS-CoV-2 could be as highly susceptible to PBL

Table 2
RT-LAMP of PBL irradiated HCoV-229E (2 μL RNA).

Sample name	Cq	Take-off
a)		
405 nm	20.03	20.60
410 nm	19.26	20.50
425 nm	17.89	19.60
450 nm	18.32	18.40
Non-irradiated Control	16.35	15.10
b) RT-LAMP of PBL irradiated HCoV-229E (4 μL RNA)		
405 nm	19.81	20.60
410 nm	19.79	20.50
425 nm	18.85	19.60
450 nm	17.65	18.40
Non-irradiated Control	16.11	15.10

inactivation as HCoV-OC43; this heightens the significance of our results. Further, since the antiviral effect of PBL was better at higher irradiances and doses, it shows that with further refinement of the treatment protocol, 100% inactivation of these coronaviruses may be attained.

Our findings have significant implications in the ongoing effort to mitigate coronavirus epidemics and pandemics, given the novelty of using blue light to inactivate coronaviruses compared to three popular ways currently used to minimize the lethality and spread of coronavirus diseases—the vaccine approach, hand washing and social distancing approach, and the use of germicidal UV. The first two approaches, vaccination, and the combination of hand-washing and social distancing effectively reduce the spread and severity of coronavirus diseases. However, they do not inactive coronaviruses, meaning that the viruses remain in the environment and society must adapt to living with coronaviruses indefinitely. The seasonal prevalence of viral diseases, such as the common cold coronavirus and flu that infected more than 105 million people and killed over 133,000 in the United States alone between 2016 and 2019 [3], even though vaccines have been available for these diseases for decades, is strong evidence that vaccines mostly enable humanity to cope with such infections.

There is a growing number of coronaviruses that humanity continues to contend with. These include SARS-CoV-1, the virus responsible for Severe Acute Respiratory Syndrome (SARS) which was first identified in February 2003 following a major outbreak in China [36], and MERS-CoV, the virus responsible for the outbreak of Middle East Respiratory Syndrome (MERS) Disease in Saudi Arabia in 2012 [37]. The prevalence of these viruses and their endemic nature clearly show that vaccines—though helpful in coping with disease—have great limitations, yet they are costly, tedious to develop, and must be refined and reinvented continually to improve their efficacy against newer strains of coronaviruses. Unlike vaccines that target individual virus strains, the probability is high that PBL can potentially inactivate current and future strains of coronaviruses, given our experience with various bacteria [16,17,32], and our present data which show that PBL inactivates two coronavirus strains—alpha coronavirus HCoV-229E and beta coronavirus HCoV-OC43. Blue light inactivates different strains of the same bacteria as well. For example, it has been shown to equally inactivate the hospital associated strain of the deadly methicillin-resistant *Staphylococcus aureus* (HA-MRSA) and the community associated strain of the same bacterium (CA-MRSA) [16,17]. Another study has shown that it eradicates two serovars of *salmonella enterica*—Typhimurium and Heidelberg as well [32].

The other contemporary approach used to contain the spread of viral infections is ultraviolet irradiation. UV is well-known to inactivate microorganisms, including coronaviruses, and it has been used for decades to disinfect lab safety hoods as well as industrial and clinical equipment used in handling infectious microorganisms. Its efficiency as a germicidal is unquestionable; however, it has several disadvantages. (1) It is carcinogenic, more so for UV-C which damages DNA than UV-B and UV-A. (2) It has a propensity to induce sunburns and skin tan, and it causes basal and squamous cell carcinomas, in particular, the UV-B wavelengths [38,39]. (3) It has a tendency to reduce the viability of keratinocytes [40–42]. (4) It causes accelerated ageing, skin wrinkling and skin melanomas over prolonged exposure periods [38]. (5) It has a penchant to damage equipment and materials made of hydrocarbon [43–45].

To limit these collateral detrimental effects of UV, recent works have focused on far UV wavelengths—215 nm to 225 nm, which are considered to be "safe." Advocates of far UV propose that it is safe for environmental disinfection even in the presence of humans because the rays are of shorter wavelength, less penetrating, and are absorbed solely in the outermost epidermis without reaching the underlying epithelium where they could be harmful [35,46–52]. Far UV-C has several advantages; (1) it is highly effective against germs. (2) It penetrates minimally in humans. (3) And it can be germicidal at ultralow fluences, all of which

suggest that its potentially harmful effects on humans may be limited. However, it does not take much irradiance for UV to cause harm because of its high photon energy. Further, the long-term effect of exposure to far UV is not known, and its tendency to degrade equipment and devices made of hydrocarbon cannot be ignored [43–45].

These observations make PBL a viable alternative germicidal that deserve further studies since: (a) microbial nucleic acids are damaged both by UV and violet-blue wavelengths, and (b) violet-blue wavelengths are safer and not known to damage hydrocarbons. Violet-blue light devices approved by the FDA in the United States have been in use and are not known to be harmful when used as recommended. This means that PBL can be deployed publicly without worrying about the type of harmful effects associated with UV. PBL is less reactive than UV, and unlike UV, it does not decompose fluids or damage plastic and rubber tubing in medical equipment and devices. This accounts for our focus on PBL instead of UV, even though UV is well-known to be anti-viral. Further, given the ubiquity of inexpensive blue LEDs, this proof-of-concept study could pave the way for novel light-based technologies that could be used to treat patients, and safely disinfect tools, equipment, hospital facilities, emergency care vehicles, airplanes, trains, cars, homes, the general environment and other spaces.

5. Conclusion

Our findings warrant the conclusion that: (1) pulsed blue light in the 405 nm to 450 nm range inactivates alpha coronavirus HCoV-229E and beta coronavirus HCoV-OC43, two coronaviruses commonly used as surrogates of SARS-CoV-2, (2) the antiviral effect of PBL is more pronounced on HCoV-OC43—a human coronavirus strain that is more closely related to SARS-CoV-2, than HCoV-229E, and (3) the antiviral effect of PBL is greater at higher irradiance and dose (12.0 mW/cm^2 and 130 J/sq. cm^2) than at lower irradiance and dose (3.0 mW/cm^2 and 32.5 J/cm^2). The latter finding suggests the need for further studies to refine the protocol with the aim of achieving 100% clearance of these and, perhaps, other viruses.

Declaration of Competing Interest

The authors declare that they have no known competing financial interests or personal relationships that could have appeared to influence the work reported in this paper.

Acknowledgements

References

[1] D.M. Morens, A.S. Fauci, The 1918 influenza pandemic: insights for the 21st century, J. Infect. Dis. 195 (2007) 1018–1028.

[2] N.P. Johnson, J. Mueller, Updating the accounts: global mortality of the 1918–1920 "Spanish" influenza pandemic, Bull. Hist. Med. 76 (2002) 105–115.

[3] Centers for Disease Control, Basic Information About SARS, 2004, pp. 1–2.

[4] Johns Hopkins University School of Medicine Coronavirus Resource Center. https://coronavirus.jhu.edu/map.html, 2021.

[5] Centers for Disease Control and Prevention, Common Colds: Protect Yourself and Others. https://www.cdc.gov/features/rhinoviruses/index.html, 2021.

[6] Centers for Disease Control and Prevention, Disease Burden of Influenza, Source: National Center for Immunization and Respiratory Diseases (NCIRD), 2020.

[7] D.L. Jarvis, A. Garcia Jr., Long-term stability of baculoviruses stored under various conditions, BioTechniques. 16 (1994) 508–513.

[8] T.B Richardson, C.D. Porter, Inactivation of murineleukaemia virus by exposure to visible light, Virology 341 (2005) 321–329.

[9] R.M. Tomb, M. Maclean, J.E. Coia, E. Graham, M. McDonald, C.D. Atreya, S. J. MacGregor, J.G. Anderson, New proof-of-concept in viral inactivation: Virucidal efficacy of 405 nm light against feline calicivirus as a model for norovirus

[10] K. Muller-Breitkreutz, H. Mohr, K. Briviba, H. Sies, Inactivation of viruses by chemically and photochemically generated singlet molecular oxygen, J. Photochem. Photobiol. 30 (1995) 63–70.

[11] B. Bachmann, J. Knuver-Hopf, B. Lambrecht, H. Mohr, Target structures for HIV-1 inactivation by methylene blue and light, J. Med. Virol. 47 (1995) 172–178.

[12] M. Schuit, S. Gardner, S. Wood, K. Bower, G. Williams, D. Freeburger, P. Dabisch, The influence of simulated sunlight on the inactivation of influenza virus in aerosols, J. Infect. Dis. 221 (2020) 372–378, https://doi.org/10.1093/infdis/jiz582.

[13] D.S. Masson-Meyers, V.V. Bumah, C. Castel, D. Castel, C.S. Enwemeka, Pulsed 450 nm blue light significantly inactivates Propionibacterium acnes more than continuous wave blue light, J. Photochem. Photobiol. B 202 (2020) 111719, https://doi.org/10.1016/j.jphotobiol.2019.111719.

[14] V.V. Bumah, D.S. Masson-Meyers, C.S. Enwemeka, Pulsed 450 nm blue light suppresses MRSA and Propionibacterium acnes in planktonic cultures and bacterial biofilms, J. Photochem. Photobiol. B 202 (2020) 111702, https://doi.org/10.1016/j.jphotobiol.2019.111702.

[15] V.V. Bumah, D.S. Masson-Meyers, W. Tong, C. Castel, C.S. Enwemeka, Optimizing the bactericidal effect of pulsed blue light on Propionibacterium acnes - a correlative fluorescence spectroscopy study, Photochem Photobiol B. 202 (2020) 111701, https://doi.org/10.1016/j.jphotobiol.2019.111701.

[16] C.S. Enwemeka, D. Williams, S. Hollosi, D. Yens, S.K. Enwemeka, Visible 405 nm SLD Photo-destroys methicillin resistant staphylococcus aureus (MRSA) in vitro, Lasers Surg. Med. 40 (2008) 734–737.

[17] C.S. Enwemeka, D. Williams, S.K. Enwemeka, S. Hollosi, D. Yens, 470 nm blue light kills methicillin resistant staphylococcus aureus (MRSA) In Vitro, Photomed. Laser Surg. 27 (2009) 221–226.

[18] N.T. De Sous, M.F. Santos, R.C. Gomes, H.E. Brandino, R. Martinez, R.R. de Jesus Guirro, Blue laser inhibits bacterial growth of Staphylococcus aureus, Escherichia coli, Pseudomonas aeruginosa, Photomed. Laser Surg. 33 (2015) 278–282.

[19] K. McKenzie, M. Maclean, I.V. Timoshkin, S.J. MacGregor, J.G. Anderson, Enhanced inactivation of Escherichia coli and listeria monocytogenes by exposure to 405 nm light under sub-lethal temperature, salt and acid stress conditions, Int. J. Food Microbiol. 17 (2013) 91–98.

[20] M.R. Hamblin, J. Viveiros, C. Yang, A. Ahmadi, A.R. Ganz, M.J. Tolkoff, Helicobacter pylori accumulates photoactive porphyrins and is killed by visible light, Antimicrob, Agents Chemother 49 (2005) 2822–2827.

[21] M. Maclean, S.J. MacGregor, J.G. Anderson, G. Woolsey, Inactivation of bacterial pathogens following exposure to light from a 405-nanometer light-emitting diode array, Appl. Environ. Microbiol. 75 (2009) 1932–1937.

[22] T. Dai, A. Gupta, Y.Y. Huang, R. Yin, C.K. Murray, M.S. Vrahas, M. Sherwood, G. P. Tegos, M.R. Hamblin, Blue light rescues mice from potentially fatal pseudomonas aeruginosa burn infection: efficacy, safety, and mechanism of action, Antimicrob. Agents Chemother. 57 (2013) 1238–1245.

[23] F. Cieplik, A. Spath, C. Leibl, A. Gollmer, J. Regensburger, L. Tabenski, K.A. Hiller, T. Maisch, G. Schmalz, Blue light kills Aggregatibacter actinomycetemcomitans due to its endogenous photosensitizers, Clin. Oral Investig. 18 (2014) 1763–1769.

[24] H. Ashkenazi, Z. Malik, Y. Harth, Y. Nitzan, Eradication of Propionibacterium acnes by its endogenic porphyrins after illumination with high intensity blue light, FEMS Immunol. Med. Microbiol. 35 (2003) 17–24.

[25] Y. Wang, R. Ferrer-Espada, Y. Baglo, Y. Gu, T. Dai, Antimicrobial blue light inactivation of Neisseria gonorrhoeae: roles of wavelength, endogenous photosensitizer, oxygen, and reactive oxygen species, Lasers Surg. Med. 51 (2019) 815–823.

[26] Y. Wang, R. Ferrer-Espada, Y. Gu, T. Dai, Antimicrobial blue light: an alternative therapeutic for multidrug-resistant gonococcal infections? MOJ Sol Photoenergy Syst. 1 (2017) 100009.

[27] Y. Wang, R. Ferrer-Espada, Y. Baglo, X.S. Goh, K.D. Held, Y.H. Grad, Y. Gu, G. A. Gelfand, T. Dai, Photoinactivation of Neisseria gonorrhoeae: a paradigm-changing approach for combating antibiotic-resistant gonococcal infection, J. Infect. Dis. 220 (2019) 873–881.

[28] O. Feuerstein, N. Persman, E.I. Weiss, Phototoxic effect of visible light on Porphyromonas gingivalis and Fusobacterium nucleatum: an in vitro study, Photochem. Photobiol. 80 (2004) 412–415.

[29] A. Yoshida, H. Sasaki, T. Toyama, M. Araki, J. Fujioka, K. Tsukiyama, N. Hamada, F. Yoshino, Antimicrobial effect of blue light using Porphyromonas gingivalis pigment, Sci. Rep. 7 (2017) 5225.

[30] E. Aboualizadeh, V.V. Bumah, D.S. Masson-Meyers, J.T. Eells, C.J. Hirschmugl, C. S. Enwemeka, Infrared microspectroscopy study: understanding the antimicrobial activity of selected disinfectants against methicillin-resistant Staphylococcus aureus (MRSA), PLoS One 12 (2017).

[31] G. Beiner, D. Masson-Meyers, V. Bumah, G. Hussey, M. Stoneman, C.S. Enwemeka, V. Raicu, Blue/violet laser inactivates methicillin-resistant Staphylococcus aureus by altering its transmembrane potential, J. Photochem. Photobiol. B 170 (2017) 118–124.

[32] V.V. Bumah, D.S. Masson-Meyers, D.S. Enwemeka, Blue 470 nm light suppresses the growth of salmonella enterica and methicillin-resistant Staphylococcus aureus (MRSA) in vitro, Lasers Surg. Med. 47 (2015) 595–601.

[33] A.R. Fehr, S. Perlman, Coronaviruses: an overview of their replication and pathogenesis, Methods Mol. Biol. 1281 (2015) 1–23.

[34] P.C.Y. Woo, Y. Huang, S.K.P. Lau, K.Y. Yuen, Coronavirus genomics and bioinformatics analysis, Viruses. 2 (2010) 1804–1820.

[35] M. Buonanno, D. Welch, I. Shuryak, D.J. Brenner, Far-UVC light (222 nm) efficiently and safely inactivates airborne human coronaviruses, Sci. Rep. 10 (2020) 10285, https://doi.org/10.1038/s41598-020-67211-2.

[36] R.H. Xu, J.F. He, M.R. Evans, G.W. Peng, H.E. Field, D.W. Yu, C.K. Lee, H.M. Luo, W.S. Lin, P. Lin, L.H. Li, W.J. Liang, J.Y. Lin, A. Schnur, Epidemiologic clues to SARS origin in China, Emerg. Infect. Dis. 10 (6) (2004) 1030–1037, https://doi.org/10.3201/eid1006.030852.

[37] A.R. Zhang, W.Q. Shi, K. Liu, et al., Epidemiology and evolution of Middle East respiratory syndrome coronavirus, 2012–2020, Infect. Dis. Poverty 10 (66) (2021), https://doi.org/10.1186/s40249-021-00853-0.

[38] K.P. Lawrence, T. Douki, R.P.E. Sarkany, S. Acker, B. Herzog, A.R. Young, The UV/visible radiation boundary region (385–405nm) damages skin cells and induces "dark" Cyclobutane pyrimidine dimers in human skin in vivo, Sci. Rep. 8 (2018) 12722.

[39] R.P. Rastogi, Richa, A. Kumar, M.B. Tyagi, R.P. Sinha, Molecular mechanisms of ultraviolet radiation-induced DNA damage and repair, J. Nucleic Acids 16 (2010) 592980.

[40] E.A. Sosnin, M.V. Erofeev, I.E. Kieft, S.E. Kunts, The effects of UV irradiation and gas plasma treatment on living mammalian cells and bacteria: a comparative approach, IEEE Tran. Plasma Sci. 32 (2004) 1544–1550.

[41] T. Dai, G.P. Tegos, T.G. St Denis, D. Anderson, E. Sinofsky, M.R. Hamblin, Ultraviolet-C irradiation for prevention of central venous catheter-related infections: an in vitro study, Photochem. Photobiol. 87 (2011) 250–255.

[42] H. Mohr, L. Steil, U. Gravemann, T. Thiele, E. Hammer, A. Greinacher, T.H. Muller, U. Volker, A novel approach to pathogen reduction in platelet concentrates using short-wave ultraviolet light, Transfusion. 49 (2009) 2612–2624.

[43] A.L. Andrady, K. Fueki, A. Torikai, Spectral sensitivity of polycarbonate to light-induced yellowing, J. Appl. Polym. Sci. 42 (1991) 2105–2107.

[44] X. Hu, Wavelength sensitivity of photooxidation of polyethylene, Polym. Degrad. Stab. 55 (1997) 131–134.

[45] A.L. Andrady, S.H. Hamid, X. Hu, A. Torikai, Effects of increased solar ultraviolet radiation on materials, J. Photochem. Photobiol. 46 (1998) 96–103.

[46] M. Buonanno, G. Randers-Pehrson, A.W. Bigelow, S. Trivedi, F.D. Lowry, H. M. Spotnitz, S.M. Hammer, D.J. Brenner, 207-nm UV light - a promising tool for safe low-cost reduction of surgical site infections. I: in vitro studies, PLoS One 8 (2013) e76968.

[47] M. Buonanno, M. Stanislauskas, B. Ponnaiya, A.W. Bigelow, G. Randers-Pehrson, Y. Xu, I. Shuryak, L. Smilenov, D.M. Owens, D.J. Brenner, 207-nm UV light-a promising tool for safe low-cost reduction of surgical site infections. II: in-vivo Safety Studies, PLoS One 11 (2–106) (2021), e0138418.

[48] M. Buonanno, B. Ponnaiya, D. Welch, M. Stanislauskas, G. Randers-Pehrson, L. Smilenov, F.D. Lowry, D.M. Owens, D.J. Brenner, Germicidal efficacy and mammalian skin safety of 222-nm UV light, Radiat. Res. 187 (2017) 483–491.

[49] K. Narita, K. Asano, Y. Morimoto, T. Igarashi, M. Hamblin, T. Dai, A. Nakane, Disinfection and healing effects of 222-nm UVC light on methicillin-resistant Staphylococcus aureus infection in mouse wounds, J. Photochem. Photobiol. B Biol. 178 (2018) 10–18.

[50] K. Narita, K. Asano, Y. Morimoto, T. Iarashi, A. Kanane, Chronic irradiation with 222-nm UVC light induces neither DNA damage nor epidermal lesions in mouse skin, even at high doses, PLoS One 13 (2018), e0201259.

[51] B. Ponnaiya, M. Buonanno, D. Welch, I. Shuryak, G. Randers-Pehrson, D. J. Brenner, Far-UVC light prevents MRSA infection of superficial wounds in vivo, PLoS One 13 (2018), e0192053.

[52] K. Narita, K. Asano, K. Naito, H. Ohashi, M. Sasaki, Y. Morimoto, T. Igarashi, A. Nakane, 222-nm UVC inactivates a wide spectrum of microbial pathogens, J. Hosp. Infect. 105 (2020) 459–467.